ChemComm

Accepted Manuscript

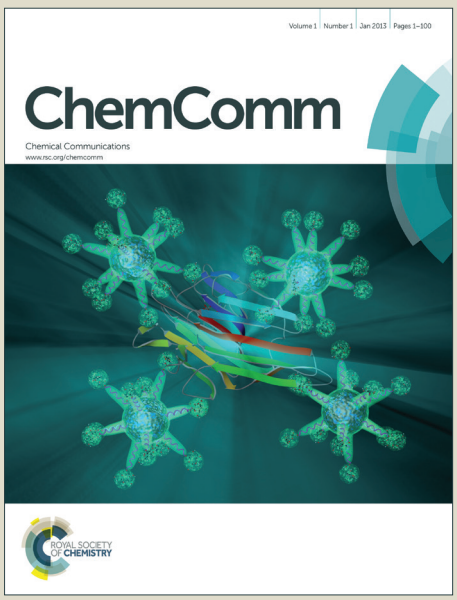

ROYAL SOCIETY OF CHEMISTRY

www.rsc.org/chemcomm

Cite this: DOI: 10.1039/c0xx00000x

www.rsc.org/xxxxxx

ARTICLE TYPE

An Interlaced Silver Vanadium Oxide-Graphene Hybrid with High Structural Stability for Use in Lithium Ion Batteries

Jiwen Qin[a‡], Wei Lv[a‡], Zhengjie Li[b], Baohua Li[a*], Feiyu Kang[a] and Quan-Hong Yang[a,b*]

Received (in XXX, XXX) Xth XXXXXXXXX 20XX, Accepted Xth XXXXXXXXX 20XX

DOI: 10.1039/b000000x

A silver vanadium oxide (SVO) material with an interlaced structure was prepared using graphene as a two-dimensional substrate that directs the crystal growth in the hydrothermal process. The obtained SVO-graphene hybrid showed high structural stability, and lithium ion batteries (LIBs) using the hybrid as the cathode had excellent cyclic stability and rate performance.

Structural stability is an essential property of a material for its use in many fields, especially in electrochemical energy storage devices such as lithium ion batteries (LIBs). LIBs store energy relying on the insertion/extraction of Li^+ in the electrode materials, which inevitably induces structure and/or volume changes, and results in capacity fade during cycling.[1] Silver vanadium oxides (SVOs) have recently been investigated as promising cathode materials for LIBs due to their remarkable electrical and ionic properties.[2] $Ag_2V_4O_{11}$, a typical example of SVOs, has been widely used as a cathode material in lithium primary batteries for implantable defibrillators because of its high energy density and long-term stability.[3] However, such SVOs have rarely been used in rechargeable LIBs due to their poor cycle and rate capability, which is attributed to the collapse of the structure of the SVOs caused by the reduction of Ag^+ during the charge/discharge process.[4] Besides, their moderate electrical conductivity also limits their applicability. [5]

Interestingly, many everyday materials with a reticulated structure, such as fabrics, have a high structural stability, which is difficult to destroy by an external force. As shown in Fig. 1, woven fabric has a strong tolerance to an external force, and only slight deformation is observed because the interlaced structure restricts the fiber network from collapse. This has inspired us to design a similar structure to stabilize electrode materials to improve their structural stability, especially for SVOs in rechargeable LIBs. As is widely reported,[6] a SVO has a belt-like structure due to its unique crystal growth, providing 'threads' that may be 'woven' into an interlaced SVO fabric. In this study, we report an interlaced structure for SVOs, which has not been previously reported since their crystal growth is usually not directed, and random aggregation always occurs for the obtained SVO belts.

In previous studies, we found that the graphene, a flat two-dimensional (2D) structure, can be used as a substrate to shape the morphology or tune the microstructure of some traditional materials, such as porous carbons and metal oxides.[7] In these cases, the key point is that metal ions and other precursors are absorbed and homogenously dispersed on the surface of graphene, and the large 2D surface prevents aggregation of the formed nanoparticles. This suggests that with the precursors pre-adsorbed on the graphene surface, SVO belt growth may be constrained along the graphene substrate to have a planar interlaced structure.

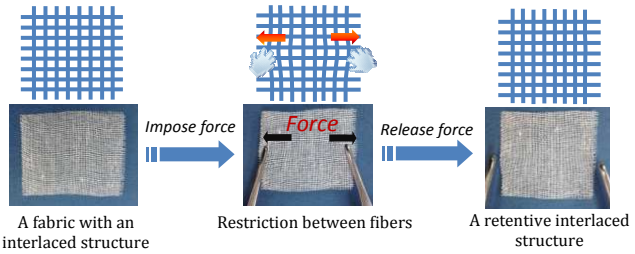

Fig. 1 Illustration of the stability of an interlaced structure.

In this study, we obtained a SVO-graphene hybrid with an interlaced structure through a simple one-step hydrothermal approach, in which a graphene substrate constrains SVO belts to grow along its planar surface, leading to the belts crossing each other and thus forming an interlaced structure. Moreover, conductive graphene acts as a micro-current collector since it binds the belts together and as a conductive additive it improves the conductivity of the obtained hybrid. As expected, such a structure effectively prevents the collapse of the electrode materials during the charge/discharge process because of a possible interlaced structure between the SVO belts and the strong adhesion between SVO belts and graphene substrates, thus providing improved cyclic stability when used as the cathode for LIBs.

The preparation process of the SVO-graphene hybrid is schematically shown in Fig. 2a. In a typical experiment, $AgNO_3$ (170 mg) was first added to a graphene oxide (GO) dispersion (40 mL, 1 mg mL^{-1}) under strong sonication to form a uniform mixed dispersion. In this process, Ag^+ was adsorbed onto the planar GO surface and the formed $AgNO_3$ particles were homogenously distributed, which is confirmed by atomic force microscopy (AFM) characterization (Fig. S1, ESI†). Then, a NH_4VO_3 (117 mg) solution was slowly added to the above mixture followed by sonication, and the obtained mixed dispersion was subjected to a hydrothermal process at 180 °C for 12 h to obtain the final SVO-graphene hybrid. The preparation details of SVO-graphene and some reference samples are presented in the Supporting Information.

Fig. 2b shows an scanning electron microscopy (SEM) image of the SVO-graphene hybrid, showing that the SVO belts form an interlaced structure. More interestingly, these belts are seen to only grow in two perpendicular directions although more detailed investigations are needed to clarify this. These belts have uniform widths in the range of 200-300 nm. In comparison, pure SVO without the graphene substrate suffers random aggregation in 3D and the belt width is non-uniform (Fig. S2, ESI†). The energy-dispersive X-ray spectroscopy (EDS) mapping demonstrates that the formed SVO-graphene hybrid is mainly composed of Ag, V and O. The carbon is hardly detected, and only a few small graphene sheets can be seen in the SEM images, which is mainly due to the low graphene content (~6%) calculated from the thermogravimetry (TG) results shown in Fig. S3 (ESI†). Another reason for the low amount of graphene detected is that the SVO belts grew directly on the graphene surface, making the covered graphene inaccessible to X-rays. Graphene sheets can be clearly

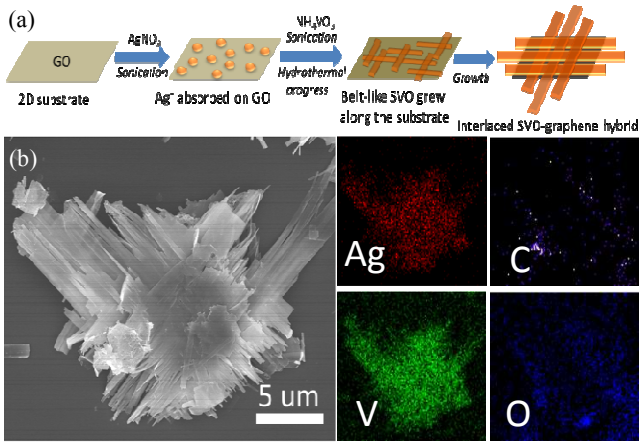

Fig. 2 (a) Schematic of the synthesis of an interlaced SVO-graphene hybrid. (b) Typical SEM image of SVO-graphene hybrid and EDS elemental mapping of Ag, V, C, O.

observed in the transmission electron microscopy (TEM) image of the SVO-graphene hybrid after sonication for the sample preparation (Fig. S4, ESI†).

In order to further demonstrate the growth process shown in Fig. 2a, we characterized the micromorphology of the hybrid prepared with different growth times, and the corresponding SEM images are shown in Fig. 3. It can be clearly observed that small particles are uniformly attached to the surface of the graphene after 1 h hydrothermal reaction (Fig. 3a) and cannot be observed outside the graphene (Fig. S1, ESI†), suggesting the reaction of Ag^+ with NH_4VO_3 occurred only on the GO surface. In the case of the 2 h reaction, these nanoparticles had grown into short ribbons and are thickly scattered on the graphene surface, forming the rudiments of an interlaced structure (Fig. 3b). For the 4 h case, these small and short ribbons had grown into larger belts along the planar graphene, resulting in a bigger and more apparent interlaced structure (Fig. 3c-d). After 12 h, a mature interlaced structure had finally been formed (Fig. 3e). Apparently, most of these belts are in two perpendicular directions. Note that a long hydrothermal reaction (e.g. 24 h) induces excessive growth of the SVO belts, resulting in severe aggregation (Fig. 3f) that is not favorable for the electrochemical applications.

The corresponding X-ray diffraction (XRD) patterns further confirm the SVO growth process. For the 1 h hydrothermal reaction, only typical peaks of Ag metal (PDF#65-2871) can be detected (Fig. S5, ESI†), which is ascribed to the high oxidation ability and instability of Ag^+ in the environment causing it to form Ag. A broad peak around 30º is observed, possibly resulting from the uncrystallized SVO. When the reaction period was increased to 2 h, the main peaks of crystalline SVO ($Ag_{1-x}V_2O_5$, PDF#18-1194) appeared, and the SVO peak intensity gradually increased with longer reaction. The hybrid prepared in the case of 12 h possesses the best crystallinity (Fig. S5, ESI†) and has a suitable structure doesn't exhibit severe aggregation (Fig. 3e), and was therefore chosen as the cathode in LIBs for the following electrochemical measurements.

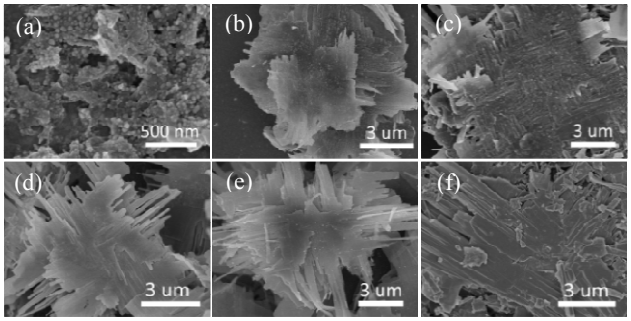

Fig. 3 Typical SEM images of SVO-graphene hybrid hydrothermally treated for (a) 1 h, (b) 2 h, (c) 4 h, (d) 8 h, (e) 12 h and (f) 24 h.

The electrochemical performance of the prepared SVO-graphene hybrid was evaluated as the cathode material in LIBs. Fig. 4a shows the cycling voltammetry (CV) curves of SVO-graphene electrode in the initial five cycles. The cathodic peaks at 2.5 V are the dominant electrochemical reactions during the Li^+ insertion derived from the reduction of V^{5+} to V^{4+} and partial V^{4+} to V^{3+}. Such peak turns into two peaks at around 2.5 V and 2.4 V after the first cycle, which may be caused by the improved activity of electrode material.[6] The other two cathodic peaks around 2.0 V and 3.0 V are ascribed to the reduction of V^{4+} to V^{3+} and Ag^+ to Ag, respectively.[8] Meanwhile, two peaks near 1.7 V and 3.2 V can also be observed, which should be attributed to the further reduction of V^{4+} to V^{3+} and a phase transformation.[8,11] All these peaks are in good agreement with the charge/discharge plateaus shown in Fig. S6. The apparent peak current density decreases after the second cycle compared to that for the first cycle, which is due to the partial irreversible transformation of Ag^+ to Ag, resulting in the crystal structure change and irreversible Li^+ insertion.[9] No obvious change is observed from the second to fifth cycles, suggesting the high stability of the SVO-graphene hybrid in this electrochemical cycling. The discharge capacity of the hybrid is ~280 mA h g^{-1} in the first cycle with a current density of 50 mA g^{-1}, and decreases to 190 mA h g^{-1} after 50 cycles. Although the capacity of the SVO without the graphene substrate shows a higher capacity for first cycle (about 290 mA h g^{-1}), it decays faster and retains a capacity of only 110 mA h g^{-1} after 50 cycles (Fig. 4b). The improved cyclic performance of the hybrid is mainly due to its high structural stability, and the interlaced structure is little changed after 50 cycles (Fig. S7, ESI†, full lithiation state). As is well known, the SVO formed without the graphene substrate is $Ag_2V_4O_{11}$ (Fig. S8, ESI†), which only has a slightly poorer cyclic stability in the electrochemical process but a higher theoretical capacity compared with $Ag_{1-x}V_2O_5$.[3] Thus, the improved cyclic performance of the hybrid must be mainly due to strong bonding between the interlaced belts lying in the two directions, either physical or chemical. Besides, graphenes also act as conductive additives and micro current collectors that bind the SVO belts together and avoid their aggregation to improve the electrochemical performance of the hybrid, which is

proved by the much lower capacity of SVO prepared by removal of graphene from SVO-graphene hybrid (Fig. S9, ESI†).

The strong interaction between the graphene sheets and SVO, which is reflected in the right shift of the G band of graphene in the Raman spectra, also contributes to the electrochemical performance improvement by promoting electron transfer. As shown in Fig. S10 (ESI†), the G band of the graphene right shifts with an increase of the hydrothermal reaction time, indicating the interaction between graphene and the formed SVO becomes stronger. The graphene-SVO interaction is also reflected by the obvious chemical shifts in C_{1s} and V_{2p} peaks of the hybrid compared with those of the simple mixture (Fig S11, ESI†).[10] Such interaction induces faster electron transfer between the SVO and graphene and the graphene also acts as both a conducting bridge and micro current collector to improve electron transfer between the SVO belts. The electrochemical impedance spectroscopy (EIS) measurements (Fig. 4c) support the above discussion. The SVO-graphene hybrid shows greatly reduced charge-transfer resistance compared with pure SVO. Moreover, as indicated by Warburg resistance results, the SVO-graphene hybrid is characterized by a low ion diffusion resistance due to low aggregation of the SVO. Both points discussed above maintain the high rate and cyclic performance of the hybrid in the electrochemical process.

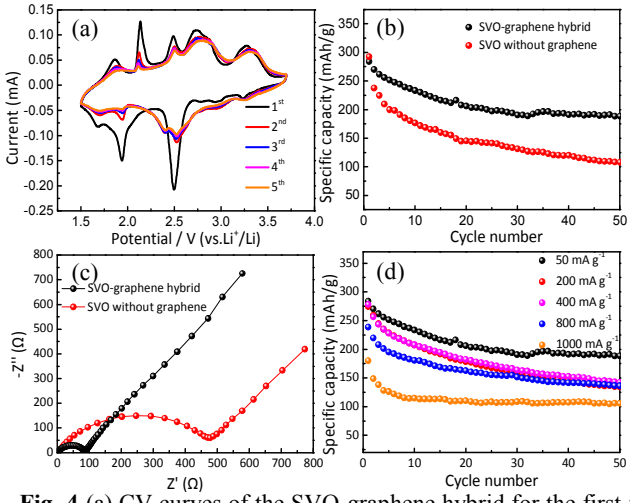

Fig. 4 (a) CV curves of the SVO-graphene hybrid for the first 5 cycles measured at a scan rate of 0.1 mV s^{-1} in the potential window 1.5-3.7 V; (b) A comparison of the cyclic stability of the SVO-graphene hybrid and SVO without graphene at 50 mA g^{-1}; (c) Nyquist plots of the SVO-graphene hybrid and SVO without graphene; (d) Rate performance of the SVO-graphene hybrid at different current densities.

Fig. 4d shows the discharge capacity of the SVO-graphene hybrid at various current densities. It can be seen that even when the current density increases to 800 mA g^{-1}, the discharge capacity is still over 150 mA h g^{-1} after 50 cycles, a value that has been rarely reported for SVO electrode materials.[11] We also investigated the influence of the amount of GO used in the preparation of SVO-graphene on the electrochemical performance of the obtained hybrids and it was found that the SVO-graphene used in this study (with an optimized GO addition amount, 40 mL 1 mg mL^{-1}, as for electrochemical performance) showed the best cyclic stability (Fig. S12, ESI†). In this case, the addition of GO greatly influences the formed SVO-graphene hybrid structure (Fig. S13, ESI†), while the crystallinity of SVO and the SVO-graphene interaction are slightly affected (Fig. S8 and S14, ESI†). A higher or lower graphene content in the hybrid induced aggregation and non-uniformity of SVO (Fig. S13, ESI†), causing an unstable secondary structure and high ion diffusion resistance (Fig. S15, ESI†). Moreover, too much graphene also hinders ion transport as demonstrated in our previous study,[12] further diminishing the electrochemical performance.

In summary, graphene is used as a substrate to direct the growth of SVO belts in a 2D platform and prevent their aggregation, and a SVO-graphene hybrid with an interlaced structure is obtained. Such a structure possesses high structural stability, and thus results in high cyclic stability and low ion transport resistance as the cathode of LIBs. Moreover, graphene also acts as a micro current collector and improves the electron transfer in electrochemical reactions in such a structure, contributing to the high rate capability. This study presents a promising and potential strategy to control the growth of the structure of non-carbon electrode materials by graphene to improve their performance and electrode stability, promoting their use in real applications.

We appreciate support from National Basic Research Program of China (2014CB932400), National Science Foundation of China (Nos. 51302146 and 51372167), NSAF (No. U1330123); Shenzhen Basic Research Project (Nos. JC201104210152A) and China Postdoctoral Science Foundation (2013T60111). We are also grateful for financial support from the Guangdong Province Innovation R&D Team Plan (No. 2009010025).

Notes and references

[a] *Engineering Laboratory for Functionalized Carbon Materials, Graduate School at Shenzhen, Tsinghua University, Shenzhen 518055, China;* yang.quanhong@sz.tsinghua.edu.cn; libh@sz.tsinghua.edu.cn.
[b] *Key Laboratory for Green Chemical Technology of Ministry of Education, School of Chemical Engineering and Technology, Tianjin University, Tianjin 300072, China;* qhyangcn@tju.edu.cn.

† Electronic Supplementary Information (ESI) available: [details of the sample preparation and characterization results of the SVO-graphene hybird and other reference samples]. See DOI:10.1039/b000000x/

‡ These two authors are equal main contributors.

1 (a) H. Li, Z. X. Wang, L. Q. Chen and X. J. Huang, *Adv Mater.* 2009, **21**, 4593; (b) J. B. Goodenough and Y. Kim, *Chem Mater.* 2010, **22**, 587; (c) C. Liu, F. Li, L. P. Ma and H. M. Cheng, *Adv Mater.* 2010, **22**, E28.
2 (a) F. Coustier, J. Hill, B. B. Owens, S. Passerini and W. H. Smyrl, *J Electrochem Soc*, 1999, **146**, 1355; (b) C. H. Han, Y. Q. Pi, Q. Y. An, L. Q. Mai, J. L. Xie, X. Xu, L. Xu, Y. L. Zhao, C. J. Niu, A. M. Khan and X. Y. He, *Nano Lett.* 2012, **12**, 4668; (c) L. Y. Liang, H. M. Liu and W. S. Yang, *Nanoscale.* 2013, **5**, 1026.
3 K. J. Takeuchi, A. C. Marschilok, S. M. Davis, R. A. Leising and E. S. Takeuchi, *Coordin Chem Rev.* 2001, **219**, 283.
4 R. P. Ramasamy, C. Feger, T. Strange and B. N. Popov, *J Appl Electrochem*, 2006, **36**, 487.
5 J. W. Lee and B. N. Popov, *J Power Sources*, 2006, **161**, 565.
6 (a) S. Q. Liang, T. Chen, A. Q. Pan, J. Zhou, Y. Tang and R. M. Wu, *J Power Sources.* 2013, **233**, 304; (b) J. M. Song, Y. Z. Lin, H. B. Yao, F. J. Fan, X. G. Li and S. H. Yu, *Acs Nano*, 2009, **3**, 653.
7 (a) W. Lv, F. Sun, D. M. Tang, H. T. Fang, C. Liu, Q. H. Yang and H. M. Cheng, *J Mater Chem*, 2011, **21**, 9014; (b) T. T. Xie, W. Lv, W. Wei, Z. J. Li, B. H. Li, F. Y. Kang and Q. H. Yang, *Chem Commun*, 2013, **49**, 10427.
8 S. Liang, J. Zhou, A. Pan, X. Zhang, Y. Tang, X. Tan, T. Chen and R. Wu, *J Power Sources*, 2013, **228**, 178.
9 C. D. Wang, Y. Li, Y. S. Chui, Q. H. Wu, X. F. Chen and W. J. Zhang, *Nanoscale*, 2013, **5**, 10599.
10 (a) G. M. Zhou, D. W. Wang, L. C. Yin, N. Li, F. Li and H. M. Cheng, *Acs Nano*, 2012, **6**, 3214; (b) J. Liu, W. Lv, W. Wei, C. Zhang, Z. Li, B. Li, F. Kang and Q. H. Yang, *J Mater Chem A*, 2014, **2**, 3031.

11 (a) L. Q. Mai, X. Xu, C. H. Han, Y. Z. Luo, L. Xu, Y. M. A. Wu and Y. L. Zhao, *Nano lett*, 2011, **11**, 4992; (b) L. Y. Liang, Y. M. Xu, Y. Lei and H. M. Liu, *Nanoscale*, 2014, **6**, 3536; (c) Y. Z. Wu, P. N. Zhu, X. Zhao, M. V. Reddy, S. J. Peng, B. V. R. Chowdari and S. Ramakrishna, *J Mater Chem A*, 2013, **1**, 852; (d) D. Wei, X. Li, Y. Zhu, J. Liang, K. Zhang and Y. Qian, *Nanoscale*, 2014, **6**, 5239.
12 F. Y. Su, Y. B. He, B. H. Li, X. C. Chen, C. H. You, W. Wei, W. Lv, Q. H. Yang and F. Y. Kang, *Nano Energy*, 2012, **1**, 429.